

**Identification of a G-Protein Subunit- $\alpha$ 11 Gain-of-Function Mutation, Val340Met, in a Family with Autosomal Dominant Hypocalcemia Type 2 (ADH2)<sup>††</sup>**

Sian E. Piret, D.Phil<sup>1\*</sup>, Caroline M. Gorvin, D.Phil<sup>1\*</sup>, Alistair T. Pagnamenta, PhD<sup>2</sup>, Sarah A. Howles, D.Phil<sup>1</sup>, Treena Cranston, BSc<sup>3</sup>, Nigel Rust, M.Phil<sup>4</sup>, M. Andrew Nesbit, PhD<sup>1,5</sup>, Ben Glaser, MD<sup>6</sup>, Jenny C. Taylor, D.Phil<sup>2</sup>, Andreas E. Buchs, MD<sup>7</sup>, Fadil M. Hannan, D.Phil<sup>1,8†</sup>, and Rajesh V. Thakker, MD<sup>1†</sup>

<sup>1</sup>Academic Endocrine Unit, University of Oxford, Oxford Centre for Diabetes, Endocrinology and Metabolism, Churchill Hospital, Headington, Oxford, OX3 7LE, UK

<sup>2</sup>Wellcome Trust Centre for Human Genetics, Roosevelt Drive, Oxford, OX3 7BN, UK; and Oxford NIHR Comprehensive Biomedical Research Centre

<sup>3</sup>Oxford University Hospitals NHS Trust, Oxford Medical Genetics Laboratories, Churchill Hospital, Headington, Oxford, OX3 7LE, UK

<sup>4</sup>Sir William Dunn School of Pathology, University of Oxford, South Parks Road, Oxford, OX1 3RE, UK

<sup>5</sup>Biomedical Sciences Research Institute, Ulster University, Coleraine, UK

<sup>6</sup>Department of Internal Medicine, Hadassah-Hebrew University Medical Center, Jerusalem, Israel

<sup>7</sup>Department of Medicine D, Assaf Harofe Medical Center, Zerifin 70300, Israel

<sup>8</sup>Department of Musculoskeletal Biology, Institute of Ageing and Chronic Disease, University of Liverpool, Daulby Street, Liverpool, L69 3GA, UK

Address correspondence to: Professor R. V. Thakker, Academic Endocrine Unit, University of Oxford, Oxford Centre for Diabetes, Endocrinology and Metabolism, Churchill Hospital, Headington, Oxford, OX3 7LE, UK. Phone: +44-1865-857501; Fax: +44-1865-857502; Email: rajesh.thakker@ndm.ox.ac.uk

\*SEP and CMG contributed equally to this work

†FMH and RVT contributed equally to this work

**Funding:** This work was supported by a Wellcome Trust Senior Investigator Award (CMG, SEP, RVT), the Medical Research Council (SEP, CMG, MAN, RVT), the National Institute for Health Research (NIHR) Oxford Biomedical Research Centre Programme (ATP, MAN, JCT), a Wellcome Trust Clinical Training Fellowship (SAH), the Wellcome Trust (ATP, JCT), and a National Institute for Health Research Senior Investigator Award (RVT). The views expressed are those of the authors and not necessarily those of the funders.

**Disclosure statement:** The authors have nothing to declare.

<sup>††</sup>This article has been accepted for publication and undergone full peer review but has not been through the copyediting, typesetting, pagination and proofreading process, which may lead to differences between this version and the Version of Record. Please cite this article as doi: [10.1002/jbmr.2797]

**Additional Supporting Information may be found in the online version of this article.**

Initial Date Submitted December 22, 2015; Date Revision Submitted January 18, 2016; Date Final Disposition Set January 22, 2016

**Journal of Bone and Mineral Research**  
**This article is protected by copyright. All rights reserved**  
**DOI 10.1002/jbmr.2797**

## Abstract

Autosomal dominant hypocalcemia (ADH) is characterized by hypocalcemia, inappropriately low serum parathyroid hormone concentrations and hypercalciuria. ADH is genetically heterogeneous with ADH type 1 (ADH1), the predominant form, being caused by germline gain-of-function mutations of the G-protein coupled calcium-sensing receptor (CaSR), and ADH2 caused by germline gain-of-function mutations of G-protein subunit  $\alpha$ -11 ( $G\alpha_{11}$ ). To date  $G\alpha_{11}$  mutations causing ADH2 have been reported in only five probands. We investigated a multi-generational non-consanguineous family, from Iran, with ADH and keratoconus which are not known to be associated, for causative mutations by whole-exome sequencing in two individuals with hypoparathyroidism, of whom one also had keratoconus, followed by cosegregation analysis of variants. This identified a novel heterozygous germline Val340Met  $G\alpha_{11}$  mutation in both individuals, and this was also present in the other 2 relatives with hypocalcemia that were tested. Three-dimensional modeling revealed the Val340Met mutation to likely alter the conformation of the C-terminal  $\alpha$ 5 helix, which may affect G-protein coupled receptor binding and G-protein activation. *In vitro* functional expression of wild-type (Val340) and mutant (Met340)  $G\alpha_{11}$  proteins in HEK293 cells stably expressing the CaSR, demonstrated that the intracellular calcium responses following stimulation with extracellular calcium, of the mutant Met340  $G\alpha_{11}$  led to a leftward shift of the concentration-response curve with a significantly ( $p < 0.0001$ ) reduced mean half-maximal concentration ( $EC_{50}$ ) value of 2.44 mM (95% CI = 2.31-2.77 mM) when compared to the wild-type  $EC_{50}$  of 3.14 mM (95% CI = 3.03-3.26 mM), consistent with a gain-of-function mutation. A novel His403Gln variant in transforming growth factor, beta-induced (TGFB1), that may be causing keratoconus was also identified, indicating likely digenic inheritance of keratoconus and ADH2 in this family. In conclusion, our identification of a novel germline gain-of-function  $G\alpha_{11}$  mutation, Val340Met, causing ADH2 demonstrates the importance of the  $G\alpha_{11}$  C-terminal region for G-protein function and CaSR signal transduction. This article is protected by copyright. All rights reserved

**Keywords:** whole-exome sequencing; G-protein; calcium; hypoparathyroidism; keratoconus

## Introduction

Autosomal dominant hypocalcemia (ADH) is a disorder of systemic calcium homeostasis that is associated with enhanced sensitivity of the calcium-sensing receptor (CaSR) to extracellular calcium ( $\text{Ca}^{2+}_o$ ) concentrations.<sup>(1-3)</sup> The CaSR is a guanine-nucleotide binding protein (G-protein)-coupled receptor (GPCR) that plays a pivotal role in  $\text{Ca}^{2+}_o$  homeostasis by transducing increases in the prevailing  $\text{Ca}^{2+}_o$  concentration into multiple signaling cascades that include  $G_{q11}$ -protein mediated activation of phospholipase C (PLC), which in the parathyroid glands and kidneys induces rapid increases in intracellular calcium ( $\text{Ca}^{2+}_i$ ) that lead to decreased parathyroid hormone (PTH) secretion and increased urinary calcium excretion, respectively.<sup>(2,4,5)</sup> ADH is a genetically heterogeneous disorder most commonly caused by germline gain-of-function mutations of the CaSR, which is encoded by the *CASR* gene on chromosome 3q21.1, and this is referred to as ADH type 1 (ADH1; OMIM #601198).<sup>(1,2,5)</sup> However, some ADH patients and families have recently been shown to harbor germline mutations of G-protein subunit- $\alpha_{11}$  ( $G\alpha_{11}$ ), which is encoded by the *GNA11* gene (Fig. 1) on chromosome 19p13.3,<sup>(3,6,7)</sup> and referred to as ADH type 2 (ADH2; OMIM #615361).<sup>(3)</sup> These ADH-associated  $G\alpha_{11}$  mutations have been demonstrated to enhance CaSR-mediated signaling in cellular studies, consistent with a gain-of-function.<sup>(3,7)</sup> ADH1 patients have calcitropic phenotypes, such as hypocalcemia with inappropriately low or normal PTH concentrations and a relative hypercalciuria that is characterised by urinary calcium to creatinine ratios that are within or above the reference range,<sup>(1,8,9)</sup> and mice with a gain-of-function CaSR mutation, that are representative of ADH1, have been reported to also have non-calcitropic phenotypes such as cataracts.<sup>(10)</sup> Although these features are similar to hypoparathyroidism, ADH1 is considered to represent a distinct disease entity from hypoparathyroidism, as affected individuals generally have PTH concentrations that are detectable and within the reference range,<sup>(1,8)</sup>. Furthermore, ADH1 patients may also develop a Bartter-like syndrome characterised by hypokalemic alkalosis, renal salt wasting and hyperreninemic hyperaldosteronism,<sup>(11,12)</sup> and the use of active vitamin D metabolites to treat symptomatic ADH1 patients may result in the development

of marked hypercalciuria, nephrocalcinosis, nephrolithiasis and renal impairment.<sup>(1,9)</sup> In contrast to ADH1, the phenotypic spectrum of ADH2 has not been fully elucidated, especially as only 5 ADH2 probands with  $G\alpha_{11}$  mutations (Fig. 1) have been reported to date.<sup>(3,6,7)</sup> Thus, it remains to be established whether ADH2 patients with germline gain-of-function  $G\alpha_{11}$  mutations are susceptible to hypercalciuria, particularly when treated with active vitamin D preparations, or at risk of a Bartter-like syndrome. Moreover,  $G\alpha_{11}$  is a widely expressed protein that mediates the biological effects of GPCRs in a range of tissues,<sup>(13)</sup> and it is currently unknown whether patients with ADH2 may harbor additional calcitropic and non-calcitropic phenotypes. We ascertained a family with ADH and keratoconus, a non-calcitropic disorder of the cornea, and hypothesized that either a single genetic abnormality may be causing ADH and keratoconus, or that ADH and keratoconus may be due to two different genetic abnormalities, i.e. digenic inheritance. To explore these hypotheses, we undertook whole-exome sequencing (WES) analysis of two relatives, both of whom had hypocalcemia, and one of whom also had keratoconus, to identify the causative variant(s).

## Materials and Methods

### Patients

The proband (individual I.4, Fig. 2A) is a 66-year-old male, from Iran, who was diagnosed with hypocalcemia at the age of 16 years following a childhood history of intermittent muscle cramps. His serum adjusted-calcium concentrations have ranged from 1.82-1.95mmol/L (normal range = 2.20-2.60 mmol/L), in association with mild hyperphosphatemia (serum phosphate = 1.42-1.81 mmol/L; normal range = 0.80-1.45 mmol/L), normal serum creatinine concentrations of 72-80  $\mu$ mol/L (normal range = 44-133  $\mu$ mol/L), low/normal serum PTH concentrations of 4.0-18.7 pg/mL (normal range = 12-65 pg/mL), a normal 25-hydroxyvitamin D concentration of 18.7 ng/ml (normal range = 10-50 ng/ml) and a normal 1,25-dihydroxyvitamin D concentration of 25.7 pg/ml (normal range = 16-45 pg/ml). He had been treated with oral calcium and active vitamin D preparations, and developed non-obstructive bilateral nephrolithiasis in association with urinary calcium values ranging from 4.3-10.2 mmol/24-hours (normal range = 2.5-7.5 mmol/24-hours). He was found to have mild bilateral cataracts at the age of 62 years. His family history revealed that 11 relatives (7 males and 4 females) over 3 generations had hypocalcemia, with symptoms such as seizures, muscle cramps, and tetany. Affected relatives also had low circulating PTH concentrations, and relative or absolute hypercalciuria (Fig. 2A), and these findings supported a diagnosis of ADH. Five hypocalcemic family members (3 males and 2 females) and one normocalcemic family member also had keratoconus, a corneal disorder, which in individuals II.3, II.5 and II.7 (Fig. 2A) had developed between the ages of 30 and 34 years.<sup>(14)</sup> There was no consanguinity and the inheritance of hypocalcemia from father to son in individuals, e.g: from I.1 to II.1 and II.2; I.4 to II.5; and II.5 to III.1 (Fig. 2A), indicated that hypocalcemia was transmitted as an autosomal dominant disorder. Similarly, the inheritance of keratoconus from father to son in individuals II.5 to III.1 (Fig. 2A), may be because keratoconus is transmitted as an autosomal dominant disorder, but the occurrence of keratoconus in the children (II.3, II.5 and II.7; and II.8) of unaffected parents (I.4 and I.5; and I.8 and I.9, respectively, Fig 2A) indicates an autosomal recessive inheritance or autosomal dominant

inheritance with reduced penetrance. To investigate the cause of the hypocalcemia and keratoconus in this family, venous blood samples were collected from four available patients, of whom two had hypocalcemia only (individuals I.4 and II.4), and two others had both hypocalcemia and keratoconus (individuals II.3 and II.5, Fig. 2A). Leucocyte DNA was extracted using the Gentra PureGene blood kit (Qiagen). CaSR mutations, which would cause ADH1, and mutations of 3 genes, *GCMB*, *PTH*, and *AIRE1*, which are known to cause hypoparathyroidism had been previously excluded by an accredited genetics diagnostic laboratory. Informed consent was obtained from all participants included in the study, using protocols approved by the UK Multicentre Research Ethics Committee (MREC/02/2/93) and the Hospital Research Ethics in Israel.

#### **Exome capture and DNA sequence analysis**

Exome capture was performed in individual I.4, who was affected with hypocalcemia, and in individual II.5, who was affected with both hypocalcemia and keratoconus (Fig. 2A), using the SeqCap EZ Human Exome Library v2.0 (Roche NimbleGen),<sup>(15)</sup> and DNA sequences determined using a 100 bp paired-end read protocol on an Illumina HiSeq2000 platform.<sup>(15)</sup> A minimum of 20x vertical read depth was obtained for >88% of the coding exome, as specified by the consensus coding sequence (CCDS) project,<sup>(16)</sup> in both individuals. Reads were aligned to the Human Sequence version 37d5 (hs37d5) reference genome using Stampy<sup>(17)</sup> and variant calling of single nucleotide variants (SNVs) and short insertions and deletions (indels) was undertaken using Platypus (v0.5.1).<sup>(18)</sup> Analysis of coding variants was undertaken using Ingenuity Variant Analysis. To search for variants causing hypocalcemia and keratoconus under autosomal dominant inheritance models, variants with a minor allele frequency (MAF) >5% within all populations of 100 genomes data (April 2012 phase 1 call set (v3 update)) and from the National Heart, Lung, and Blood Institute (NHLBI) exome sequencing project (Exome Variant Server, NHLBI GO Exome Sequencing Project (ESP), Seattle, WA (evs.gs.washington.edu/EVS), were excluded. To search

Accepted Article

for variants causing keratoconus under an autosomal recessive inheritance model, variants with a MAF >5% were not excluded. The pathogenicity of variants was inferred from several criteria: allele frequency within the NHLBI exome sequencing project and the Exome Aggregation Consortium (ExAC), Cambridge, MA (<http://exac.broadinstitute.org>), amino acid conservation, physicochemical alterations in amino acid substitutions, splice site prediction algorithms (NNSPLICE ([http://www.fruitfly.org/seq\\_tools/splice.html](http://www.fruitfly.org/seq_tools/splice.html)), MaxEntScan ([http://genes.mit.edu/burgelab/maxent/Xmaxentscan\\_scoreseq.html](http://genes.mit.edu/burgelab/maxent/Xmaxentscan_scoreseq.html)), GeneSplicer ([http://www.cbcb.umd.edu/software/GeneSplicer/gene\\_spl.shtml](http://www.cbcb.umd.edu/software/GeneSplicer/gene_spl.shtml)) and SpliceSiteFinder-Like (<http://www.genet.sickkids.on.ca/~ali/splicesitefinder.html>)), and literature review. Variants of interest were confirmed by polymerase chain reaction (PCR) and Sanger DNA sequence analysis of the appropriate exons, using leucocyte DNA samples from the 4 available family members and 2 unrelated unaffected individuals, as reported.<sup>(19)</sup>

### Protein sequence alignments and three-dimensional modeling

Amino acid sequences of  $G\alpha$ -subunit paralogs and TGFBI orthologs were aligned using the Clustal Omega program (European Bioinformatics Institute, the European Molecular Biology Laboratory). The crystal structure of  $G\alpha_q$  in complex with the GTP analogue GDP-AIF<sub>4</sub> has been determined (Protein Data Bank (PDB) accession number 3OHM),<sup>(20)</sup> and this was used to model  $G\alpha_{11}$ , which has 90% identity with  $G\alpha_q$  at the amino acid level, using the PyMOL Molecular Graphics System (Version 1.2r3pre, Schrodinger, LLC).

### Cell Culture and Transfection

The generation of wild-type and mutant Leu341 pBI-CMV2-*GNA11* expression constructs have been reported.<sup>(3)</sup> Site-directed mutagenesis was used to generate the Val to Met mutation at codon 340 in the pBI-CMV2-*GNA11* construct using the Quikchange Lightning Site-directed Mutagenesis kit (Agilent Technologies) and gene-specific primers (SigmaAldrich), as reported.<sup>(19)</sup> For all

studies, empty vector, wild-type or mutant pBI-CMV2-*GNA11* expression constructs were transiently transfected into human embryonic kidney (HEK) 293 cells stably expressing the CaSR (HEK293-CaSR) using Lipofectamine 2000 (LifeTechnologies).<sup>(21)</sup> Cells were maintained in DMEM-Glutamax media (ThermoFisher) with 10% fetal bovine serum (Gibco) and 400µg/mL geneticin (ThermoFisher) at 37°C, 5% CO<sub>2</sub>. Successful transfection was confirmed by visualising GFP fluorescence using an Eclipse E400 fluorescence microscope with a Y-FL Epifluorescence attachment and a triband 4,6-diamidino-2-phenylindole-FITC-Rhodamine filter, and images captured using a DXM1200C digital camera and NIS Elements software (Nikon).<sup>(3,21,22)</sup> The expression of Gα<sub>11</sub> and CaSR proteins was also determined by Western blot analysis using anti-Gα<sub>11</sub> (SantaCruz), anti-GFP (SantaCruz), anti-calnexin (Millipore) or anti-CaSR (Abcam) antibodies. The Western blots were visualized using Immuno-Star WesternC kit (BioRad) on a BioRad Chemidoc XRS+ system.<sup>(3)</sup>

### **Intracellular Calcium Measurements**

The Ca<sup>2+</sup><sub>i</sub> responses of HEK293-CaSR cells expressing wild-type or mutant Gα<sub>11</sub> proteins were assessed by a flow cytometry-based assay, as reported.<sup>(2,3,21,22)</sup> In brief, HEK293-CaSR cells were plated in T75 flasks and transiently transfected 24 hours later with 16µg DNA.<sup>(3)</sup> At 48-hours post-transfection, cells were detached, resuspended in calcium (Ca<sup>2+</sup>) and magnesium (Mg<sup>2+</sup>) free Hanks' buffered saline solution (HBSS) and loaded with 1µg/mL Indo-1-acetoxymethylester (Indo-1-AM) for 1 hour at 37°C. After removal of free dye, the cells were resuspended in Ca<sup>2+</sup> and Mg<sup>2+</sup>-free HBSS and maintained at 37°C. Transfected cells, in suspension, were analysed by flow cytometry on a MoFlo modular flow cytometer (Beckman Coulter) and data on the Ca<sup>2+</sup><sub>i</sub> responses to alterations in Ca<sup>2+</sup><sub>o</sub> collected from all cells that expressed GFP, by simultaneous measurements of GFP expression (at 525nm), Ca<sup>2+</sup><sub>i</sub>-bound Indo-1AM (at 410nm), and free Indo-1AM (i.e. not bound to Ca<sup>2+</sup><sub>i</sub>) (at 485nm), using a JDSU Xcyte laser (Coherent Radiation), on each cell at each Ca<sup>2+</sup><sub>o</sub> concentration [Ca<sup>2+</sup>]<sub>o</sub>, as described.<sup>(3,21)</sup> Assays were performed in four biological replicates for



each of the expression constructs. The peak mean fluorescence ratio of the transient response after each individual stimulus was measured using Cytomation Summit software (Beckman Coulter), and expressed as a normalised response, as previously described.<sup>(3,21)</sup> Nonlinear regression of concentration-response curves was performed with GraphPad Prism using the normalised response at each  $[Ca^{2+}]_o$  for each separate experiment for the determination of the  $EC_{50}$  (i.e.,  $[Ca^{2+}]_o$  required for 50% of the maximal response). Data is presented as mean with confidence interval or mean  $\pm$  standard error of the mean (SEM). Statistical analysis was performed using the F-test. A value of  $p < 0.05$  was considered significant for all analyses.

## Results

### Identification of a novel Val340Met $G\alpha_{11}$ mutation

Exome capture and high-throughput sequence analysis of genomic DNA from two affected individuals, one with hypocalcemia (individual I.4) and the other with hypocalcemia and keratoconus (individual II.5) (Fig. 2A) resulted in the detection of >5,000 non-dbSNP variants in both individuals. The exclusion of variants with a MAF of >5% resulted in the identification of 104 novel variants in 103 genes, of which three variants were excluded as sequence artefacts as they occurred within trinucleotide repeats. The only variant identified in a gene previously associated with hypocalcemia, was a heterozygous G>A transition at nucleotide c.1018 (c.1018G>A), located in exon 7 of the *GNA11* gene (Fig. 1). The variant was confirmed by Sanger DNA sequencing to be present in both patients affected with hypocalcemia (individuals I.4 and II.5) and in two other family members (individuals II.3 and II.4) with hypocalcemia from whom samples were available (Fig. 2B). This G>A transition (GTG to ATG) resulted in a missense substitution, Val340Met, of the encoded  $G\alpha_{11}$  protein (Fig. 2C). The absence of this DNA sequence abnormality in >60,000 exomes from the Exome Aggregation Consortium (ExAC), together with evolutionary conservation of the Val340 residue in vertebrate  $G\alpha$ -subunit paralogs (Fig. 3A) indicated that the Val340Met abnormality likely represented a pathogenic *GNA11* mutation rather than a benign polymorphic variant.

### Identification of candidate variant for keratoconus

Whole-exome sequencing revealed a novel heterozygous c.1209T>G transversion in *TGFBI*, encoding a variant His403Gln in transforming growth factor beta-induced (TGFBI), which was present in both individuals (I.4 and II.5, Fig. S1A). The TGFBI His403Gln variant is not present in ExAC, although a different variant in the same amino acid, His403Tyr, is present in only 3 out of >60,000 individuals. The His403 residue is also evolutionarily conserved in TGFBI orthologs (Fig. S1B). The *TGFBI* variant was confirmed by Sanger DNA sequence analysis in the siblings, II.3 and

II.5, who had hypocalcemia and keratoconus, but its absence in the sister II.4, who has hypocalcemia only, indicates that this TGFBI variant is not involved in the etiology of hypocalcemia (Fig. S1A). Moreover, the presence of this TGFBI variant in the father (individual I.4), who was affected with hypocalcemia only, indicates likely non-penetrance of the mutant allele (Fig. S1A).

### **Structural characterisation of the Val340Met $G\alpha_{11}$ mutant protein**

To evaluate whether the Val340Met *GNA11* variant represents a pathogenic mutation and the cause of hypocalcemia in this family, structural and functional studies were undertaken. The crystal structure of  $G\alpha_q$ , which shares 90% amino acid identity with  $G\alpha_{11}$ ,<sup>(3,20)</sup> was used to predict the effects of the Val340Met mutation. The mutated Val340 residue is located within the  $\alpha 5$  helix of the GTPase domain of  $G\alpha_{11}$  (Fig. 3B-C), and next to the Phe341 residue, which has been reported to be associated with a gain-of-function Phe341Leu mutation (Fig. 1 and 3B) causing ADH2.<sup>(3)</sup> The  $\alpha 5$  helix is located at the C-terminus of  $G\alpha$ -subunits and plays a critical role in GPCR binding and G-protein activation.<sup>(23,24)</sup> Indeed, the C-terminal portion of the  $\alpha 5$  helix, which is known as the interface module, directly binds to the transmembrane domain and intracellular loops of activated GPCRs,<sup>(24)</sup> whilst the N-terminal portion, which is known as the transmission module, interacts with the GTPase domain  $\beta$ -sheet, comprising the  $\beta 1$ - $\beta 6$  strands (Fig. 3C), to mediate conformational changes in  $G\alpha$ -subunit structure that facilitate guanine nucleotide exchange.<sup>(23,25)</sup> The Val340 residue is predicted to form non-polar interactions with the conserved Phe272 and His327 residues, located in the  $\beta 5$  and  $\beta 6$  strands, respectively (Fig. 3C), which are considered to stabilize the binding of G-protein with ligand-bound GPCR.<sup>(23,25,26)</sup> The Val340Met mutation is predicted to impair the interaction with the His327  $G\alpha_{11}$  residue (Fig. 3D), thereby altering the conformation of the  $\alpha 5$  helix and/or  $\beta 6$  strand, and destabilizing the  $G\alpha$ -GPCR complex.

### **Functional characterisation of the Val340Met $G\alpha_{11}$ mutant protein**

To determine the effects of these predicted changes in  $G\alpha_{11}$  structure (Fig. 3) on CaSR-mediated signaling, bidirectional pBI-CMV2-*GNA11* expression constructs containing wild-type (WT) Val340, mutant Met340, or the previously reported gain-of-function Leu341 mutant *GNA11* cDNA,<sup>(3)</sup> or vector containing the green fluorescence protein (GFP) reporter gene alone were transiently transfected into HEK293 cells stably expressing the CaSR. Expression of CaSR,  $G\alpha_{11}$  and GFP was confirmed by fluorescence microscopy and/or Western blot analysis (Fig. 4A-B). Calnexin was used as a loading control in Western blot analyses, and  $G\alpha_{11}$  expression was demonstrated to be similar in cells transiently transfected with wild-type or mutant  $G\alpha_{11}$  proteins, and greater than that of cells transfected with the empty pBI-CMV2 vector (Fig. 4B). The responses of  $[Ca^{2+}]_i$  to alterations in  $[Ca^{2+}]_o$  in cells expressing the different *GNA11* vectors were assessed by flow cytometry. The  $Ca^{2+}_i$  responses in wild-type and mutant  $G\alpha_{11}$ -expressing cells were shown to increase in a dose-dependent manner following stimulation with increasing concentrations of  $Ca^{2+}_o$  between 0-15 mM. However, expression of the Met340 and Leu341 mutant  $G\alpha_{11}$  proteins resulted in a leftward shift of the concentration-response curves (Fig. 4C), with significantly lower half maximal ( $EC_{50}$ ) values, compared to wild-type Val340  $G\alpha_{11}$  and empty vector (Met340 = 2.44 mM (95% confidence interval (CI) = 2.31-2.77 mM); Val340 = 3.14 mM (95% CI = 3.03-3.26 mM); empty vector = 3.12mM (95% CI = 2.99-3.25 mM);  $p < 0.0001$ ) (Fig. 4D). There was no significant difference in the  $EC_{50}$  values between Met340 and Leu341 (Leu341 = 2.60mM (95% CI = 2.49-2.72 mM);  $p > 0.05$ ). Thus, the Val340Met missense substitution represents a novel gain-of-function  $G\alpha_{11}$  mutation, similar to those reported in ADH2 patients.<sup>(3,7)</sup>

## Discussion

The identification of a germline gain-of-function  $G\alpha_{11}$  mutation, Val340Met, indicates ADH2 to be the likely cause of hypocalcemia in this family. To date, five other hypocalcemic patients and families have been reported to harbor germline  $G\alpha_{11}$  mutations, consistent with a diagnosis of ADH2.<sup>(3,6,7)</sup> Similar to the family characterized in this study, individuals with germline gain-of-function  $G\alpha_{11}$  mutations have been reported to generally have mild-to-moderate hypocalcemia (serum adjusted-calcium concentrations ranging from 1.75-2.15 mmol/L) in association with serum PTH concentrations that are detectable and within the lower half of the normal range.<sup>(3,6,7)</sup> However, despite ADH2 being associated with mild biochemical features, affected individuals are commonly symptomatic and may present with paraesthesia, muscle cramps, carpo-pedal spasms or seizures.<sup>(3,6,7)</sup> Moreover, as described for the proband in this study (individual I.4, Fig. 2A), some ADH2 patients appear susceptible to treatment-related hypercalciuria, nephrocalcinosis and nephrolithiasis,<sup>(7)</sup> although affected individuals likely have a milder urinary phenotype, with significantly reduced urinary calcium excretion compared to ADH1 patients who harbor gain-of-function CaSR mutations.<sup>(7)</sup> Furthermore, patients with germline heterozygous gain-of-function  $G\alpha_{11}$  mutations, in contrast to patients with germline heterozygous gain-of-function CaSR mutations, may have non-calcitropic phenotypes. For example, short stature caused by postnatal growth insufficiency was reported in affected individuals from a multi-generational kindred with hypocalcemia and a germline heterozygous gain-of-function mutation, Arg60Leu,<sup>(7)</sup> and it is possible that the occurrence of mild bilateral cataracts in the proband (individual I.4) may also be due to the germline gain-of-function  $G\alpha_{11}$  mutation, Val340Met. It is also of interest to note that somatic  $G\alpha_{11}$  mutations that lead to constitutive G-protein activation are associated with the development of uveal melanomas.<sup>(27)</sup> However, keratoconus, a corneal disorder, was not observed in all patients harboring the germline Val340Met  $G\alpha_{11}$  mutation, thereby indicating that keratoconus is not due to the  $G\alpha_{11}$  mutation. Instead, keratoconus in this family is likely due to the identified novel germline variant, His403Gln in TGFBI (Fig. S1), abnormalities of which have

previously been reported in association with keratoconus and autosomal dominant forms of corneal dystrophy.<sup>(28,29)</sup> Thus, the occurrence of keratoconus and ADH2 in this family are not genetically associated, but are instead due to digenic inheritance of mutations involving TGFBI and  $G\alpha_{11}$ .

Structural and functional studies of ADH2-causing gain-of-function  $G\alpha_{11}$  mutations have revealed residues and peptide motifs critical for  $G\alpha$ -subunit function. Thus, the importance of the interface at which the  $G\alpha$ -subunit helical and GTPase domains interact to mediate guanine nucleotide exchange, has been demonstrated by the reported Arg60Leu, Arg60Cys and Arg181Gln  $G\alpha_{11}$  mutations,<sup>(3,6,7)</sup> which are located at the interdomain interface (Fig. 3B),<sup>(25)</sup> and predicted to disrupt GDP binding.<sup>(3,6,7)</sup> Whereas, the reported ADH2-causing Ser211Trp mutation, located in the  $\alpha 2$  helix of the GTPase domain (Fig. 3B), may cause a gain-of-function by dissociating the  $G\alpha$ -subunit from the  $G\beta\gamma$  heterodimer.<sup>(6)</sup> Furthermore, the reported ADH2-causing Phe341Leu mutation<sup>(3)</sup> is located in the C-terminal  $\alpha 5$  helix, which facilitates G-protein-GPCR coupling<sup>(23)</sup>, and the mutated Phe341 residue is predicted to play major roles in G-protein activation and inactivation.<sup>(25,26)</sup> Indeed, under basal conditions, Phe341 forms part of a hydrophobic cluster of phenylalanine residues that maintains the  $G\alpha$ -subunit in an inactive GDP-bound conformation.<sup>(25,26)</sup> Upon ligand-binding, Phe341 binds to the second intracellular loop of the activated cognate GPCR,<sup>(24)</sup> which disrupts the hydrophobic cluster, leading to the release of GDP.<sup>(25,26)</sup> The Phe341Leu mutation is predicted to affect the hydrophobic cluster,<sup>(3)</sup> thereby leading to GDP/GTP exchange and G-protein activation. In contrast to these roles of Phe341, the neighboring Val340 residue does not bind to activated GPCRs and is not involved in GDP/GTP exchange,<sup>(24,25)</sup> but instead may play a role in stabilizing the nucleotide-free conformation of the  $G\alpha$ -subunit once bound to activated GPCR.<sup>(23)</sup> Thus, the Val340Met mutation likely mediates  $G\alpha_{11}$  activation by influencing the stability of  $G\alpha$ -GPCR interactions. These different ADH2 mutations have yielded insights into  $G\alpha$ -subunit structure-function relationships, which may aid the design of novel targeted therapeutic agents for the treatment of ADH, for which there is currently a lack of adequate drugs.<sup>(30)</sup>

In conclusion, we have identified a novel germline gain-of-function  $G\alpha_{11}$  mutation, Val340Met, that causes ADH2 in a family in which some members also suffered from keratoconus. Keratoconus in this family was likely due to a novel germline TGFBI His403Gln variant, thereby indicating that keratoconus and ADH2 are not caused by the same mutation, but instead the combined occurrence of ADH2 and keratoconus in some family members is due to digenic inheritance. Finally our study provides an exemplar of the clinical utility of WES, that enabled the identification of two likely genetic causes by a single experimental protocol, which would not have been readily possible using former genetic techniques.

## Acknowledgments

This work was supported by a Wellcome Trust Senior Investigator Award (CMG, SEP, RVT), the Medical Research Council (SEP, CMG, MAN, RVT), the National Institute for Health Research (NIHR) Oxford Biomedical Research Centre Programme (ATP, MAN, JCT), a Wellcome Trust Clinical Training Fellowship (SAH), the Wellcome Trust (ATP, JCT), and a National Institute for Health Research Senior Investigator Award (RVT). The views expressed are those of the authors and not necessarily those of the funders.

**Authors' roles:** Study design: SEP, CMG, ATP, JCT, FMH, and RVT. Data collection: SEP, CMG, ATP, SAH, TC, NR, BG, and AB. Data analysis: SEP, CMG, ATP, SAH, TC, and NR. Data interpretation: SEP, CMG, ATP, SAH, TC, NR, MAN, JCT, FH, and RVT. Drafting manuscript, revising manuscript content, and approving final version of manuscript: SEP, CMG, ATP, SAH, TC, NR, MAN, BG, JCT, AEB, FMH, and RVT.



## References

1. Pearce SH, Williamson C, Kifor O, et al. A familial syndrome of hypocalcemia with hypercalciuria due to mutations in the calcium-sensing receptor. *N Engl J Med* 1996;335(15):1115-1122.
2. Hannan FM, Nesbit MA, Zhang C, et al. Identification of 70 calcium-sensing receptor mutations in hyper- and hypo-calcaemic patients: evidence for clustering of extracellular domain mutations at calcium-binding sites. *Hum Mol Genet* 2012;21(12):2768-2778.
3. Nesbit MA, Hannan FM, Howles SA, et al. Mutations affecting G-protein subunit alpha11 in hypercalcemia and hypocalcemia. *N Engl J Med* 2013;368(26):2476-2486.
4. Hofer AM, Brown EM Extracellular calcium sensing and signalling. *Nat Rev Mol Cell Biol* 2003;4(7):530-538.
5. Hannan FM, Thakker RV Calcium-sensing receptor (CaSR) mutations and disorders of calcium, electrolyte and water metabolism. *Best Pract Res Clin Endocrinol Metab* 2013;27(3):359-371.
6. Mannstadt M, Harris M, Bravenboer B, et al. Germline mutations affecting Galpha11 in hypoparathyroidism. *N Engl J Med* 2013;368(26):2532-2534.
7. Li D, Opas EE, Tuluc F, et al. Autosomal dominant hypoparathyroidism caused by germline mutation in GNA11: phenotypic and molecular characterization. *J Clin Endocrinol Metab* 2014;99(9):E1774-1783.
8. Raue F, Pichl J, Dorr HG, et al. Activating mutations in the calcium-sensing receptor: genetic and clinical spectrum in 25 patients with autosomal dominant hypocalcaemia - a German survey. *Clin Endocrinol (Oxf)* 2011;75(6):760-765.
9. Yamamoto M, Akatsu T, Nagase T, Ogata E Comparison of hypocalcemic hypercalciuria between patients with idiopathic hypoparathyroidism and those with gain-of-function mutations in the calcium-sensing receptor: is it possible to differentiate the two disorders? *J Clin Endocrinol Metab* 2000;85(12):4583-4591.

10. Hough TA, Bogani D, Cheeseman MT, et al. Activating calcium-sensing receptor mutation in the mouse is associated with cataracts and ectopic calcification. *Proc Natl Acad Sci U S A* 2004;101(37):13566-13571.
11. Vargas-Poussou R, Huang C, Hulin P, et al. Functional characterization of a calcium-sensing receptor mutation in severe autosomal dominant hypocalcemia with a Bartter-like syndrome. *J Am Soc Nephrol* 2002;13(9):2259-2266.
12. Watanabe S, Fukumoto S, Chang H, et al. Association between activating mutations of calcium-sensing receptor and Bartter's syndrome. *Lancet* 2002;360(9334):692-694.
13. Wettschureck N, Offermanns S Mammalian G proteins and their cell type specific functions. *Physiol Rev* 2005;85(4):1159-1204.
14. Vazirani J, Basu S Keratoconus: current perspectives. *Clin Ophthalmol* 2013;7:2019-2030.
15. Taylor JC, Martin HC, Lise S, et al. Factors influencing success of clinical genome sequencing across a broad spectrum of disorders. *Nat Genet* 2015;47(7):717-726.
16. Pruitt KD, Harrow J, Harte RA, et al. The consensus coding sequence (CCDS) project: Identifying a common protein-coding gene set for the human and mouse genomes. *Genome Res* 2009;19(7):1316-1323.
17. Lunter G, Goodson M Stampy: a statistical algorithm for sensitive and fast mapping of Illumina sequence reads. *Genome Res* 2011;21(6):936-939.
18. Rimmer A, Phan H, Mathieson I, et al. Integrating mapping-, assembly- and haplotype-based approaches for calling variants in clinical sequencing applications. *Nat Genet* 2014;46(8):912-918.
19. Newey PJ, Gorvin CM, Cleland SJ, et al. Mutant prolactin receptor and familial hyperprolactinemia. *N Engl J Med* 2013;369(21):2012-2020.
20. Waldo GL, Ricks TK, Hicks SN, et al. Kinetic scaffolding mediated by a phospholipase C-beta and Gq signaling complex. *Science* 2010;330(6006):974-980.

21. Nesbit MA, Hannan FM, Howles SA, et al. Mutations in AP2S1 cause familial hypocalciuric hypercalcemia type 3. *Nat Genet* 2013;45(1):93-97.
22. Hannan FM, Howles SA, Rogers A, et al. Adaptor protein-2 sigma subunit mutations causing familial hypocalciuric hypercalcaemia type 3 (FHH3) demonstrate genotype-phenotype correlations, codon bias and dominant-negative effects. *Hum Mol Genet* 2015;24(18):5079-5092.
23. Flock T, Ravarani CN, Sun D, et al. Universal allosteric mechanism for G $\alpha$  activation by GPCRs. *Nature* 2015;524(7564):173-179.
24. Rasmussen SG, DeVree BT, Zou Y, et al. Crystal structure of the beta2 adrenergic receptor-Gs protein complex. *Nature* 2011;477(7366):549-555.
25. Sun D, Flock T, Deupi X, et al. Probing G $\alpha$  protein activation at single-amino acid resolution. *Nat Struct Mol Biol* 2015;22(9):686-694.
26. Kaya AI, Lokits AD, Gilbert JA, Iverson TM, Meiler J, Hamm HE A conserved phenylalanine as a relay between the alpha5 helix and the GDP binding region of heterotrimeric Gi protein alpha subunit. *J Biol Chem* 2014;289(35):24475-24487.
27. Van Raamsdonk CD, Griewank KG, Crosby MB, et al. Mutations in GNA11 in uveal melanoma. *N Engl J Med* 2010;363(23):2191-2199.
28. Guan T, Liu C, Ma Z, Ding S The point mutation and polymorphism in keratoconus candidate gene TGFBI in Chinese population. *Gene* 2012;503(1):137-139.
29. Stewart HS, Ridgway AE, Dixon MJ, Bonshek R, Parveen R, Black G Heterogeneity in granular corneal dystrophy: identification of three causative mutations in the TGFBI (BIGH3) gene-lessons for corneal amyloidogenesis. *Hum Mutat* 1999;14(2):126-132.
30. Hannan FM, Walls GV, Babinsky VN, et al. The Calcilytic Agent NPS 2143 Rectifies Hypocalcemia in a Mouse Model With an Activating Calcium-Sensing Receptor (CaSR) Mutation: Relevance to Autosomal Dominant Hypocalcemia Type 1 (ADH1). *Endocrinology* 2015;156(9):3114-3121.

## Figure legends

**Fig. 1.** Schematic representation of the genomic organisation of the human *GNA11* gene showing the location of ADH2-causing mutations. The *GNA11* gene consists of 7 exons with the start (ATG) and stop (TGA) codons located in exons 1 and 7, respectively. The GTPase domain (encoded by exon 1, 5' portion of exon 2, 3' portion of exon 4 and exons 5-7) is connected to the helical domain (encoded by the 3' portion of exon 2, exon 3, and 5' portion of exon 4) by the linker 1 (L1) and linker 2 (L2) peptides. The previously reported ADH2-causing Arg60Cys (R60C), Arg60Leu (R60L) and Arg181Gln (R181Q) mutations<sup>(3,6,7)</sup> are located at the interface between the helical and GTPase domains and adjacent to the linker peptides. The reported ADH2-causing Ser211Trp (S211W) mutation is located in the  $\alpha 2$  helix of the GTPase domain,<sup>(6)</sup> and the Val340Met (V340M) mutation reported by this study (shown in bold), and the previously reported Phe341Leu (F341L) mutation<sup>(3)</sup> are located in the  $\alpha 5$  helix of the GTPase domain. Coding-regions are shaded gray and untranslated regions are represented by open boxes.

**Fig. 2.** Identification of a Val340Met  $G\alpha_{11}$  mutation in a family with hypocalcemia and keratoconus. (A), Pedigree of the family, with males and females indicated by squares and circles, respectively. Individuals affected with hypocalcemia, keratoconus or the combined occurrence of hypocalcemia and keratoconus are indicated by left half-filled, right half-filled or filled symbols, respectively, and unaffected individuals are indicated by open symbols. The proband (individual I.4) is indicated by an arrow, and asterisks indicate those individuals from whom DNA was available for these studies. Plasma calcium (Ca) (mmol/L; normal range = 2.20-2.60 mmol/L) and plasma PTH (pg/ml; normal range = 12-65 pg/ml) values are shown for individuals I.4, II.3, II.4 and II.5. (B), A heterozygous G>A transition at nucleotide c.1018 within exon 7 of *GNA11* (Fig. 1) was identified by WES and confirmed by Sanger DNA sequence analysis. The c.1018G>A *GNA11* variant was detected in all 4 family members with hypocalcemia from whom samples were

available. (C), This DNA sequence abnormality was predicted to lead to a missense amino acid substitution of Val to Met at codon 340.

**Fig. 3.** Predicted effects of the Val340Met mutation on the  $G\alpha_{11}$  protein. (A), Multiple protein sequence alignment of residues comprising the  $\alpha 5$  helix of  $G\alpha$ -subunit paralogs. The wild-type Val340 (V) and mutant Met340 (M) residues are shown in bold. Conserved residues are shaded gray. (B), Overall three-dimensional structure of the  $G\alpha_{11}$  protein. The  $G\alpha$ -subunit helical (blue) and GTPase (green) domains are connected by the L1 and L2 peptides (gray). The five  $G\alpha_{11}$  residues, which have been reported to be mutated in ADH2,<sup>(3,6,7)</sup> are shown in magenta. The mutated Arg60 and Arg181 residues are located at the interdomain interface (red dashed line), which forms a pocket for the binding of guanine nucleotides (yellow). The GTPase domain is the location of the mutated Ser211 residue ( $\alpha 2$  helix), and mutated Val340 and Phe341 residues ( $\alpha 5$  helix). (C), Close-up view of the  $\alpha 5$  helix, which comprises a C-terminal interface module (pink) that interacts with partner GPCRs and an N-terminal transmission module (purple), which interacts with the surrounding  $\beta 1$ - $\beta 6$  strands to facilitate conformational changes that lead to guanine nucleotide exchange and  $G\alpha$ -subunit activation.<sup>(23)</sup> The wild-type Val340 residue (red) is predicted to form non-polar interactions with the Phe272 and His327 residues (cyan),<sup>(26)</sup> which are located in the  $\beta 5$  and  $\beta 6$  strands, respectively. (D), The introduction of a mutant Met340 residue (red, space filling model) is predicted to sterically hinder His327 (cyan, stick model), thereby altering the conformation of the  $\alpha 5$  helix and/or  $\beta 6$  strand.

**Fig. 4.** Functional characterisation of wild-type and ADH2-associated mutant  $G\alpha_{11}$  proteins. (A), Fluorescence microscopy of HEK293 cells stably expressing CaSR (HEK293-CaSR) and transiently transfected with wild-type (WT) or ADH2-associated mutant (Met340 and Leu341) *GNA11*-pBI-CMV2-GFP constructs, or with vector (V) only. Detection of GFP in these cells indicates successful transfection and expression of these constructs. Bar indicates 10 $\mu$ m. (B),

Western blot analysis of whole cell lysates using antibodies to CaSR, calnexin,  $G\alpha_{11}$  and GFP.

Transient transfection of WT or ADH2-associated mutant constructs resulted in over-expression of

$G\alpha_{11}$  when normalized to calnexin expression. (C), Concentration-response curves showing

normalized  $Ca^{2+}_i$  response to changes in  $[Ca^{2+}]_o$  of HEK293-CaSR cells transfected with WT or

ADH2-associated  $G\alpha_{11}$  mutants. The  $Ca^{2+}_i$  responses are shown as the mean  $\pm$  SEM of 4

independent transfections. The ADH2-associated  $G\alpha_{11}$  mutants (Met340 and Leu341) led to a

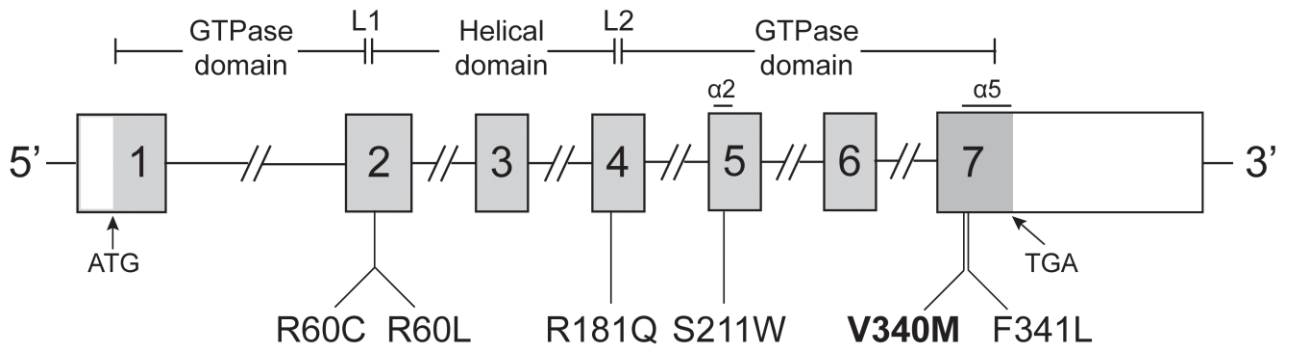
leftward shift of the concentration-response curves (blue and red, respectively) when compared with

WT  $G\alpha_{11}$  (black), which harbors Val and Phe residues at codons 340 and 341, respectively. (D),

The Met340 and Leu341 mutants (blue and red bars, respectively) were associated with

significantly decreased  $EC_{50}$  values compared to cells expressing WT  $G\alpha_{11}$  (black bar).

\*\*\* $p < 0.0001$ .

**Figure 1**

**Figure 2**

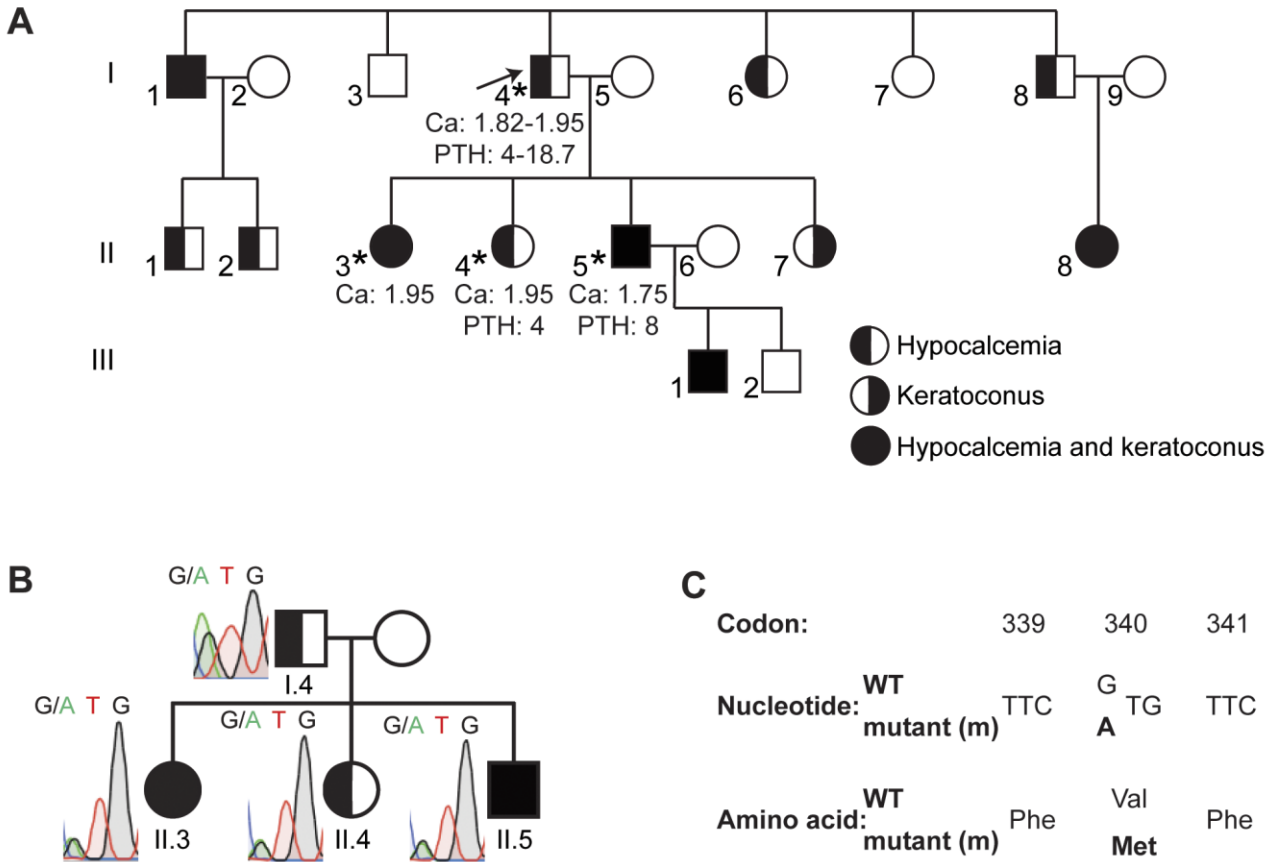
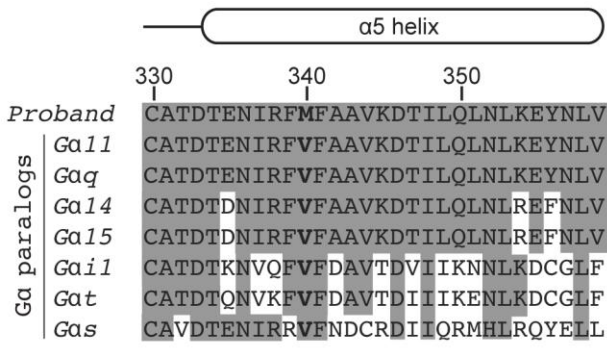


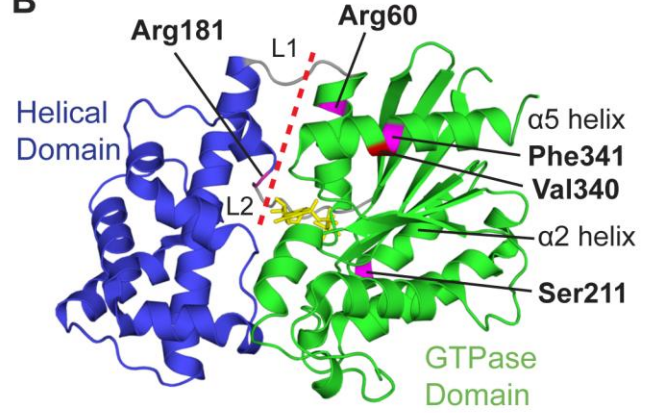


**Figure 3**

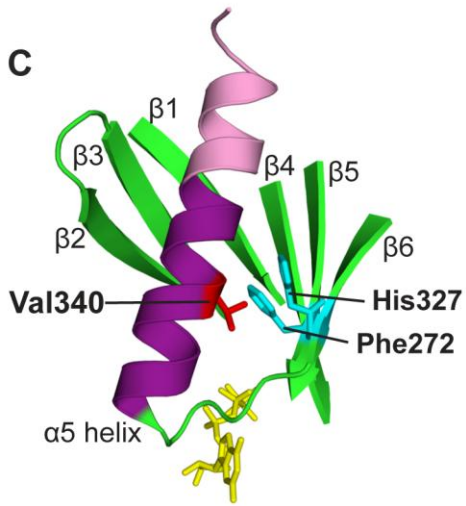
**A**



**B**



**C**



**D**

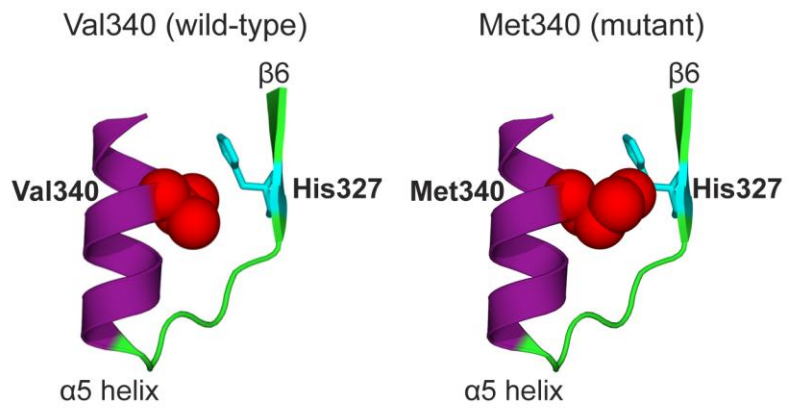


**Figure 4**

